Kinetics of the Reactions of CH_2I, CH_2Br, and CHBrCl Radicals with NO_2 in the Temperature Range 220−360 K

Arkke J. Eskola,[†] Dorota Wojcik-Pastuszka,[‡] Emil Ratajczak,[‡] and Raimo S. Timonen*[,†]

Laboratory of Physical Chemistry, P.O. Box 55 (A.I. Virtasen aukio 1), FIN-00014 University of Helsinki, Finland, and Department of Physical Chemistry, Medical University of Wroclaw, pl Nankiera 1, 50-140 Wroclaw, Poland

Received: July 4, 2006; In Final Form: September 5, 2006

The kinetics of the $CH_2I + NO_2$, $CH_2Br + NO_2$, and $CHBrCl + NO_2$ reactions have been studied at temperatures between 220 and 360 K using laser photolysis/photoionization mass spectrometry. Decays of radical concentrations have been monitored in time-resolved measurements to obtain reaction rate coefficients under pseudo-first-order conditions. The bimolecular rate coefficients of all three reactions are independent of the bath gas (He or N_2) and pressure within the experimental range (2−6 Torr) and are found to depend on temperature as follows: $k(CH_2I + NO_2) = (2.18 \pm 0.07) \times 10^{-11} (T/300\ K)^{-1.45 \pm 0.22}$ cm^3 molecule^{-1} s^{-1} (220−363 K), $k(CH_2Br + NO_2) = (1.76 \pm 0.03) \times 10^{-11} (T/300\ K)^{-0.86 \pm 0.09}$ cm^3 molecule^{-1} s^{-1} (221−363 K), and $k(CHBrCl + NO_2) = (8.81 \pm 0.28) \times 10^{-12} (T/300\ K)^{-1.55 \pm 0.34}$ cm^3 molecule^{-1} s^{-1} (267−363 K), with the uncertainties given as one-standard deviations. Estimated overall uncertainties in the measured bimolecular reaction rate coefficients are about ±25%. In the $CH_2I + NO_2$ and $CH_2Br + NO_2$ reactions, the observed product is formaldehyde. For the $CHBrCl + NO_2$ reaction, the product observed is CHClO. In addition, I atom and iodonitromethane (CH_2INO_2) or iodomethyl nitrite (CH_2IONO) formations have been detected for the $CH_2I + NO_2$ reaction.

Introduction

The reactions of carbon-centered free radicals with nitrogen dioxide are highly exothermic and generally have high rate coefficients. For example, Geppert et al.,[1] who recently studied the kinetics of the reactions of vinyl (C_2H_3) and propargyl (C_3H_3) radicals with NO_2 using a flow reactor combined with a photoionization mass spectrometer, report room-temperature reaction rate coefficients of $(4.2 \pm 0.8) \times 10^{-11}$ cm^{-3} s^{-1} and $(2.6 \pm 0.5) \times 10^{-11}$ cm^{-3} s^{-1} for these species, respectively. For comparison, the highly reactive vinyl radical reacts about 40 times faster than the resonance-stabilized propargyl radical with molecular oxygen under the same conditions.[2−5] This is much larger difference than the above ∼ 40% in the reactions with NO_2. Platz et al.[6] have studied the kinetics of phenoxy radical (C_6H_5O) reaction with O_2 and NO_2 employing FTIR/smog chamber method and pulse radiolysis/UV absorption technique. Both experiments have been performed at room temperature and at about atmospheric pressure. For the O_2 reaction, they were able to obtain very low upper limit, $k(C_6H_5O + O_2) < 5 \times 10^{-21}$ cm^{-3} s^{-1}, while the measured value under the same conditions for the NO_2 reaction was $k(C_6H_5O + NO_2) = (2.08 \pm 0.15) \times 10^{-12}$ cm^{-3} s^{-1}. Due to the extremely low reactivity of C_6H_5O with O_2, the loss of phenoxy radical in moderately polluted urban air ([$NO_x \approx 1-10$ ppbv]) is thus not the reaction with O_2 but for example with NO_2. The resonance-stabilized phenoxy radical is, in part, a carbon-centered free radical[6] and is thus relevant to the present study.

To obtain deeper understanding of the reasons affecting the reactivity of radicals, it is profitable to systemically investigate series of reactions in which only one parameter (e.g. radical substitution) is changed at a time.[7] For example, Eskola et al.[8] have recently studied the kinetics of chlorinated methyl radical (CH_2Cl, $CHCl_2$, and CCl_3) reactions with NO_2 at temperatures between 220 and 360 K using the flow reactor combined with the photoionization mass spectrometer. They observed a clear decreasing trend of reactivity from the CH_2Cl to the CCl_3 radical at room temperature. At each step the substitution of hydrogen atom by the chlorine atom decreases the rate coefficient about 60%. No evidence of activation barriers or pressure dependencies was observed in any of these reactions. In the present study we continue the systematic work among the reactions of halogen-substituted alkyl radicals with NO_2 and we describe the first direct experimental rate measurements for reactions 1−3.

$$CH_2I + NO_2 \rightarrow \text{products} \quad (1)$$

$$CH_2Br + NO_2 \rightarrow \text{products} \quad (2)$$

$$CHBrCl + NO_2 \rightarrow \text{products} \quad (3)$$

While few reactions have been studied fairly intensively, especially $CH_2OH + NO_2$ and $CF_3 + NO_2$, the number of substituted methyl radical reactions with nitrogen dioxide subjected to direct studies is small. Nesbitt et al.[9] have investigated the reaction of hydroxymethyl radical (CH_2OH) with NO_2 at low pressures (∼1 Torr He) using a discharge-flow system combined with a mass spectrometer and obtained a bimolecular rate coefficient $(8.3 \pm 2.1) \times 10^{-12}$ cm^{-3} s^{-1} at room temperature. Pagsberg et al.[10] have studied the same reaction at room temperature and atmospheric pressure obtaining a rate coefficient $(2.3 \pm 0.4) \times 10^{-11}$ cm^{-3} s^{-1} using pulse

* To whom correspondence should be addressed: raimo.timonen@helsinki.fi.
[†] University of Helsinki.
[‡] University of Wroclaw.

10.1021/jp064197e CCC: $33.50
Published on Web 10/17/2006

radiolysis to generate radicals and UV absorption technique to measure the kinetics. They also observed the formation of a long-lived or stable product. Combining this finding with their larger rate coefficient at atmospheric pressure, they concluded that the difference between the two rate coefficient values is probably due to the effect of bath gas pressure on stabilizing the adducts. Breheny et al. (see ref 11 for other studies of this reaction) have investigated the $CF_3 + NO_2$ reaction at room temperature and over the pressure range 1.5−110 Torr of Ar and N_2 using time-resolved infrared emission spectroscopy and obtained a bimolecular rate coefficient $(1.75 \pm 0.26) \times 10^{-11}$ cm^{-3} s^{-1}. These results and a work of Sillesen et al.[12] employing pulse radiolysis/UV absorption technique indicate that the main channel yields FNO and CF_2O products. However, at higher pressures, the formation of the adduct might have some minor importance.[11] Slagle et al.[13] have studied the $CF_2Cl + NO_2$ reaction at room temperature and at low pressure (∼1 Torr He) and obtained a rate coefficient $(9.6 \pm 1.9) \times 10^{-12}$ cm^{-3} s^{-1} using the flow reactor combined with the photoionization mass spectrometer. Employing the same technique under similar conditions, Park et al.[14] have obtained rate coefficients $(4.5 \pm 0.9) \times 10^{-11}$ cm^{-3} s^{-1} and $(1.9 \pm 0.4) \times 10^{-11}$ cm^{-3} s^{-1} for the $C_2H_5 + NO_2$ and $CH_2CN + NO_2$ reactions, respectively. Finally, the temperature dependencies of the substituted methyl radical reactions with NO_2 studied in direct time-resolved measurements are only available for the above-mentioned chlorinated methyl radical reactions with NO_2.

Experimental Section

Details of the experimental apparatus and procedures used have been described previously,[3,8] so only a brief overview is given here. The radical R (R = CH_2I, CH_2Br, or CHBrCl) was generated from an appropriate precursor at 193 or 248 nm along the flow reactor by pulsed unfocused exciplex laser (ELI-76E) photolysis. The gas mixture flowing through the tubular, temperature-controlled reactor coupled with the photoionization mass spectrometer (PIMS) contained the radical precursor (<0.15%), NO_2 in varying amounts (<0.05%), and an inert carrier gas (He or N_2) in large excess (>99.8%). The employed reactor tubes with 8 and 17 mm inner diameters (i.d.) were made of seamless stainless steel and were coated with halocarbon wax. The gas flow rates at used pressures (2−6 Torr of He or N_2) and temperatures (220 K to 363 K) were typically about 4−5 ms^{-1} inside the reactor, which means that the gas mixture passes the uniformly cooled (heated) zone in about 80 ms. The gas was continuously sampled through a 0.4 mm diameter hole at the side of the reactor and formed into a beam by a conical skimmer before it entered a vacuum chamber containing PIMS. As the gas beam traversed the ion source, a portion was selectively photoionized and the ions formed were mass selected in a quadrupole mass spectrometer (Extrel, C-50/150-QC/19 mm rods). The selected ions were detected by an off-axis electron multiplier.

Ionization radiation in the PIMS was provided by atomic resonance lamps: a Cl-lamp (8.9−9.1 eV) for CH_2I, CH_2Br, and CHBrCl, an H-lamp (10.2 eV) for CH_2Br, CHBrCl, CH_2IO, CH_2BrO, $CHBrClO$, CH_2IONO_2, CH_2INO_2, CH_2BrONO_2, $CHBrClONO_2$, CH_2BrNO_2, $CHBrClNO_2$, HNO, BrNO, INO, IO, I, CHIO, HIO, HI, HBrO, BrO, and NO, an Ar-lamp (11.6−11.8 eV) for CD_2O, CH_2BrNO_2, and HBrO, and a Ne-lamp (16.7−16.9 eV) for HBr, HNO_2, ClO, BrO, Br, Cl, HBrO, CHClO, $CHBrClNO_2$, BrNO, and CHBrO. The CH_2Br and CHBrCl radical decays were mainly measured with the Cl-lamp, while a few profiles were obtained with the H-lamp. However, no differences in the decay profiles were observed. Temporal ion signals were recorded by a multichannel scaler (EG&G Ortec MCS plus) from 10 ms before each laser pulse up to 80 ms following the pulse. Typically, a profile from 3000 to 10000 repetitions was accumulated at about 5 Hz frequency before the nonlinear least-squares method was used to fit an exponential function, $[R]_t = [R]_0 \times \exp(-k't)$, to the data. Here $[R]_t$ is the signal proportional to the radical concentration at time t, and k' is the first-order rate coefficient.

The CH_2I radicals were generated either from CH_2ICl[15] as

$$CH_2ICl + h\nu(193\ nm) \rightarrow CH_2I + Cl \quad (4a)$$

$$\rightarrow CH_2Cl + I/I^* \quad (4b)$$

$$\rightarrow \text{other products} \quad (4c)$$

or from CH_2I_2[16,17] (CD_2I_2) as

$$CH_2I_2\ (CD_2I_2) + h\nu(248\ nm) \rightarrow CH_2I\ (CD_2I) + I \quad (5a)$$

$$\rightarrow CH_2I\ (CD_2I) + I^* \quad (5b)$$

$$\rightarrow \text{other products} \quad (5c)$$

The CH_2Br radicals were produced either from CH_2BrI[17,18] as

$$CH_2BrI + h\nu(248\ nm) \rightarrow CH_2Br + I/I^* \quad (6a)$$

$$\rightarrow \text{other products} \quad (6b)$$

or from CH_2Br_2[17,19] (CD_2Br_2) as

$$CH_2Br_2\ (CD_2Br_2) + h\nu(248\ nm) \rightarrow CH_2Br\ (CD_2Br) + Br \quad (7a)$$

$$\rightarrow \text{other products} \quad (7b)$$

while CHBrCl radicals were produced from $CHBr_2Cl$[20] as

$$CHBr_2Cl + h\nu(248\ nm) \rightarrow CHBrCl + Br \quad (8a)$$

$$\rightarrow \text{other products} \quad (8b)$$

Deuterated diiodomethane (CD_2I_2) or dibromomethane (CD_2Br_2) was used as a precursor instead of CH_2I_2 or CH_2Br_2 in order to avoid contribution from NO (m = 30 u, IE (ionization energy) = 9.26 eV),[21] when the formation of the formaldehyde as a product ($m(CH_2O)$ = 30 u, $m(CD_2O)$ = 32 u and IE ≈ 10.9 eV for both)[21] was measured.

Experiments were conducted under conditions where only two significant reactions consumed R:

$$R + NO_2 \rightarrow \text{products} \quad (A)$$

$$R \rightarrow \text{heterogeneous loss} \quad (B)$$

The first-order decay rate of the reaction B (the wall reaction rate coefficient k_{wall}) consists of all first-order processes occurring in the reaction mixture and on the reactor wall without the added molecular reactant. It was measured by reducing the precursor concentration and/or laser intensity until the rate obtained for this reaction no longer depended on these factors and the exponential fit to the temporal ion signal showed no deviation from the first-order decay. When these conditions were achieved, it was presumed that all radical−radical processes were suppressed (i.e. these had negligible rates compared to the first order processes occurring in the system). Initial R concentrations were then typically below 3×10^{11} cm^{-3}, which

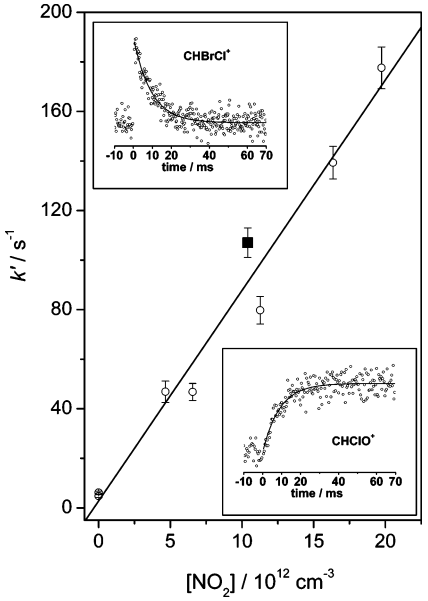

Figure 1. Plot of the first-order CHBrCl rate coefficient k' vs $[NO_2]$ at $T = 298$ K and $P = 5$ Torr in an 8 mm i.d. reactor tube. Insets show ion signal profiles for the CHBrCl decay and CHClO formation under the conditions of the solid square in the plot: $[NO_2] = 1.0 \times 10^{13}$ cm^{-3}, $k'_{decay}(CHBrCl) = 107 \pm 7$ s^{-1}, $k'_{rise}(CHClO) = 112 \pm 7$ s^{-1}, and $k_{wall} = 6 \pm 1$ s^{-1}. Uncertainties are one-standard deviations (1σ).

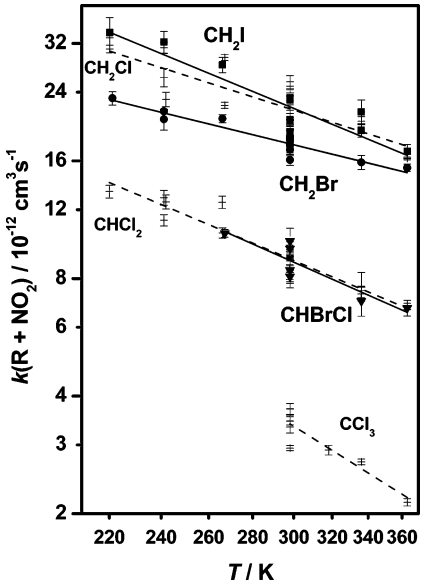

Figure 2. Double-logarithmic plots of bimolecular rate coefficients for the current (CH_2I, CH_2Br, and CHBrCl) and previous[8] (CH_2Cl, $CHCl_2$, and CCl_3) radical reactions with NO_2 versus T. The current data are shown with filled symbols and fittings with solid lines. Values from the previous measurements are given for comparison and are shown with cross symbols and fittings with dashed lines.

was estimated from the laser fluences and known absorption cross-sections of the precursors at used wavelengths.

The first-order rate coefficient (k') was then measured as a function of the NO_2 concentration ($[NO_2]$), which was always much higher (>15 times) than [R], resulting in pseudo-first-order reaction kinetics. Since the only significant processes consuming R during these experiments were the reaction with NO_2 (A) and disappearance in the heterogeneous reaction (B), the bimolecular reaction rate coefficient $k(R + NO_2)$ could be obtained from the slope of the k' vs $[NO_2]$ plot. A typical plot is shown in Figure 1 for the CHBrCl + NO_2 reaction. An example of the CHBrCl radical signal decay is inserted in the upper left corner of the Figure 1.

Radical precursors, CH_2ICl (Aldrich, purity >97%), CH_2I_2 (Fluka, purity ≥ 98%), CD_2I_2 (Aldrich, purity >99%), CH_2BrI (Aldrich), CH_2Br_2 (Fluka, purity >99%), CD_2Br_2 (Aldrich, purity >99%), $CHBr_2Cl$ (Aldrich, purity 98%), and NO_2 (Merck, purity 98%), were degassed before use. The NO_2 gas was diluted in He to form about 10% mixture and was stored in a blackened glass bulb. Helium (Messer-Griesheim purity of 99.9996%) and nitrogen (Aga purity of 99.9999%) were employed as supplied.

Results and Discussion

The measured bimolecular reaction rate coefficients for the CH_2I, CH_2Br, and CHBrCl radical reactions with NO_2 are given in Table 1 with their statistical uncertainties (1σ) and experimental conditions. Estimated overall uncertainties in measured bimolecular reaction rate coefficients are about ± 25%. These arise mainly from the uncertainties in determining the reactant concentrations and from the uncertainties in the first-order rate coefficients. Linear least-squares fits of an expression $k = A \times (T/300\ K)^n$ to the experimental results are also given in Table 1. In this expression T is temperature in K, and A and n are empirical parameters. Double-logarithmic plots of the bimolecular rate coefficients for the CH_2I, CH_2Br, and CHBrCl radical reactions with NO_2 are shown in Figure 2. Also shown are values from the previous study[8] ($CH_2Cl + NO_2$, $CHCl_2 + NO_2$, and $CCl_3 + NO_2$) for comparison.

Similar to our previous studies with NO_2,[1,8] investigations were also performed in the current work to exclude possible problems in the kinetic measurements, which this reactant might cause. The unimolecular decomposition[22,23] rate of N_2O_4 is about 1000 s^{-1} at 295 K and 8 torr pressure, i.e. under conditions in which reactant flow rates were measured employing pressure increase in a known volume. Due to the very short lifetime of N_2O_4 under these conditions, in comparison to the time the pressure increase is followed in the flow rate measurements, equilibrium from concentrated mixture to dilute can be said to be reached very rapidly. According to the equilibrium thermodynamics,[23,24] under conditions of the source bulb (~295 K, ~760 Torr, and 10% NO_2 in He) about 42% of NO_2 is in a form of N_2O_4, and this fraction decreases to about 1.2% in a measuring volume and still further after mixing with carrier gas until in the reactor inlet this fraction is below 0.1%. Consequently, only the total concentration of NO_2 in the source bulb (N_2O_4 in equilibrium with NO_2 counted twice) is needed and can be calculated using equilibrium thermodynamics. Although traces of N_2O_4 are still available in the reactor and absorption cross-section of N_2O_4 is significantly larger than that of NO_2 at both 193 and 248 nm, only NO_2 molecules, in different states of excitation, are formed in the N_2O_4 photolysis.[25,26] In addition, equilibrium is not reached within the short residence time (~100 ms) in the cooled zone of the reactor because the recombination rate for dimer formation ($k' \approx 0.05$ s^{-1}) is slow under experimental conditions.[22,23] It can be summarized that due to the small concentrations of NO_2 used for kinetic studies in this work, very small amounts of dimers in equilibrium with monomers do not have any significant effect on our results.

Investigations were also performed to observe the possible presence of second-order heterogeneous wall reactions. Both small (8 mm) and large (17 mm) id reactor tubes with the same coatings were employed to vary the surface-to-volume ratio.[3,27] One would expect a larger bimolecular reaction rate coefficient $k(R + NO_2)$ for the smaller tube, if second order heterogeneous reactions occurred in any significant extent. This was not observed and only the first-order wall reaction rate coefficient

TABLE 1: Results and Conditions of the Experiments[a] Used To Measure the Bimolecular Rate Coefficients of the Reaction R + NO_2 → Products (R = CH_2I, CH_2Br, and CHBrCl)

T/K	P[b]/Torr	$10^{-12}[NO_2]$/cm^{-3}	d[c]$_{reactor}$/ mm	k_{wall}/s^{-1}	$10^{12}k$[d]/cm^3 s^{-1}
		R = CH_2I			
		$k(CH_2I + NO_2) = (2.18 \pm 0.07)\ 10^{-11}\ (T/300\ K)^{-1.45 \pm 0.22}$ cm^3 s^{-1}			
220	3.9	2.6−10.5	8	44	34.1 ± 3.1
241	4.5	2.2−10.1	8	32	32.3 ± 2.1
266	5.0	2.8−13.8	8	28	28.2 ± 1.3
298[e]	5.1	2.3−13.3	8	9	18.9 ± 1.0
298[e]	2.0[f]	2.5−13.6	8	6	20.3 ± 0.5
298[e]	2.3[g]	2.4−16.8	8	6	20.4 ± 1.2
298[e]	5.0[h]	2.2−13.9	8	7	22.9 ± 0.7
298[i]	4.9	3.0−11.7	8	17	24.8 ± 1.1
298[e]	2.5	1.8−9.4	17	5	18.5 ± 0.9
298	4.9	4.9−12.4	8	25	23.2 ± 0.5
336[e]	5.8	2.6−14.0	8	6	19.2 ± 0.8
336	4.9	1.9−10.2	8	15	21.4 ± 1.6
363[e]	5.0	1.7−9.8	8	15	16.9 ± 0.7
		R = CH_2Br			
		$K(CH_2Br + NO_2) = (1.76 \pm 0.03)\ 10^{-11}\ (T/300\ K)^{-0.86 \pm 0.09}$ cm^3 s^{-1}			
221	3.7	2.2−12.0	8	13	23.2 ± 1.0
241	2.2	1.7−14.9	17	6	20.5 ± 1.3
241	4.1	2.6−13.5	8	9	21.4 ± 0.3
266	4.5	2.2−11.3	8	9	20.5 ± 0.5
298	2.0[f]	2.2−9.7	8	8	17.6 ± 0.8
298	2.4	2.2−15.9	8	7	17.1 ± 0.6
298	2.5	1.5−12.4	17	3	18.1 ± 0.6
298[j]	4.9	5.1−19.7	8	7	16.1 ± 0.6
298[k]	4.8	3.0−14.0	8	10	19.8 ± 0.8
298	5.1[l]	2.3−20.5	8	8	17.6 ± 0.3
298	5.0[m]	2.5−21.2	8	8	18.4 ± 0.3
336	5.8	2.7−17.0	8	10	15.9 ± 0.7
363	6.2	2.4−14.3	8	10	15.4 ± 0.4
		R = CHBrCl			
		$k(CHBrCl + NO_2) = (8.81 \pm 0.28)\ 10^{-12}\ (T/300\ K)^{-1.55 \pm 0.34}$ cm^3 s^{-1}			
267	4.6	4.7−18.9	8	7	10.4 ± 0.3
298	2.0[f]	4.1−14.0	8	8	9.98 ± 0.8
298	2.4	4.3−16.7	8	6	8.09 ± 0.6
298	2.4	6.5−24.8	17	3	9.54 ± 0.4
298	5.0	4.7−19.7	8	5	8.41 ± 0.6
336	5.9	5.2−21.5	8	6	7.01 ± 0.6
363	6.3	4.7−18.6	8	10	6.72 ± 0.4

[a] Range of precursor concentrations used: (0.6−2.2) × 10^{12} molecule cm^{-3} for CH_2ICl, (0.7−7.4) × 10^{12} molecule cm^{-3} for CH_2I_2 (CD_2I_2), (1.1−4.6) × 10^{13} molecule cm^{-3} for CH_2Br_2 (CD_2Br_2), 1.5 × 10^{13} molecule cm^{-3} for CH_2BrI, and (1.0−4.0) × 10^{13} molecule cm^{-3} for $CHBr_2Cl$. Laser intensities used were 5.7−15 mJ/cm^2 (193 nm) and 5.9−45 mJ/cm^2 (248 nm). Estimated initial radical R concentrations were 0.4−4.0 × 10^{11} molecule cm^{-3}. [b] Helium used as a buffer gas unless otherwise stated. [c] Reactor inner diameter. Coated with halocarbon wax. [d] Statistical uncertainties shown are 1σ; estimated overall uncertainty is ±25%. [e] CH_2I_2 used as a precursor. [f] Nitrogen used as a buffer gas. [g,h] In case of *h* laser intensity (∼45 mJ cm^{-2}) was about 6 times higher and precursor concentration (∼7 × 10^{11} molecule cm^{-3}) correspondingly lower than in case of *g* (∼7 mJ cm^{-2} and ∼34 × 10^{11} molecule cm^{-3}). [i] CD_2I_2 used as a precursor. [j] CH_2BrI used as a precursor. [k] CD_2Br_2 used as a precursor. [l,m] In case of *l* laser intensity (∼38 mJ cm^{-2}) was about 3 times higher and precursor concentration (∼1.1 × 10^{13} molecule cm^{-3}) correspondingly lower than in case of *m*(∼12 mJ cm^{-2} and ∼4.6 × 10^{13} molecule cm^{-3}).

k_{wall} was larger for the smaller tube. We concluded that second-order wall reactions are unimportant in our experiments.

Some NO_2 was photolyzed in the laser pulse at 193 or 248 nm according to the following reactions:[28,29]

$$NO_2 + h\nu(193\ nm) \rightarrow NO + 0.55\ O(^1D) + 0.45\ O(^3P) \quad (9)$$

$$NO_2 + h\nu(248\ nm) \rightarrow NO + O(^3P) \quad (10)$$

Experiments were mainly performed with relatively high precursor concentrations but with low laser intensities (an average about 9 mJcm^{-2} at 193 nm and about 20 mJcm^{-2} at 248 nm) to minimize NO_2 decomposition. Oxygen atom concentration was typically in the range 0.5−2 × 10^{10} molecule cm^{-3}, which was estimated from the absorption cross-section of NO_2[28,29] and the measured laser intensity. A few measurements were carried out with lower precursor concentrations and higher laser intensities to test the possible importance of radical-precursor reactions. For the $CH_2I + NO_2$ reaction at 298 K using CH_2I_2 precursor with 248 nm photolysis, about 6 times higher laser intensity (∼45 mJ cm^{-2}, see *g,h* in Table 1) and correspondingly lower precursor concentration did not cause any changes in k_{wall} and no effect on $k(R + NO_2)$ within estimated overall uncertainties of ±25%. A similar observation was also made for the $CH_2Br + NO_2$ reaction at 298 K using CH_2Br_2 precursor with 248 nm photolysis (see *l,m* in Table 1). Measurements performed using either N_2 or He as buffer gas yielded the same bimolecular reaction rate coefficients within experimental error, which rules out disturbing effects on kinetics caused by excited oxygen atoms [$O(^1D)$], because under experimental conditions nitrogen quenches the excitation already within the first 10 μs after the photolysis pulse.[23]

After completing the investigations of reaction 1, it was noticed that measurements performed with the CH_2I_2 precursor

produced bimolecular reaction rate coefficients, which were systemically slightly smaller (or equal) than results obtained with the CH_2ICl precursor. One possible explanation could be $O(^3P) + CH_2I_2$ reaction, for which Teruel et al.[30] have obtained temperature independent reaction rate coefficient $k(O(^3P) + CH_2I_2) = (7.36 \pm 0.47) \times 10^{-11}$ cm^{-3} s^{-1} by employing laser photolysis−resonance fluoresence technique. Unfortunately, no information on the yield of the CH_2I radical in this reaction is available. Thus it is possible that small concentration of oxygen atoms formed in the photodissociation of NO_2 could generate some CH_2I radicals from the CH_2I_2 precursor. However, although the $[O]_0/[CH_2I]_0$ ratio was varied between 0.05 and 0.4, no systematic decrease in the measured bimolecular reaction rate coefficients as the function of this ratio, due to the regeneration of CH_2I radicals, was observed. Also, the values of the bimolecular rate coefficients of the $CH_2I + NO_2$ reaction obtained at the same temperature with either CH_2I_2 or CH_2ICl as the precursor are all well within the estimated overall uncertanty of ±25%. Consequently, data from all measurements were used in the fitting process.

Formaldehyde (or CD_2O when CD_2I_2 was used as a precursor) was detected as a product of the $CH_2I/CD_2I + NO_2$ reaction. In addition, a relatively weak signal for the formation of iodonitromethane (CH_2INO_2) or iodomethyl nitrite (CH_2IONO) product was observed (CH_2ICl was used as a precursor in this case). Search of products of the reaction 1 were mainly performed using diiodomethane as the precursor because in the 248 nm photodissociation of the CH_2I_2, only a weak signal of the HI was observed in addition to the strong signals of the CH_2I radical and I atom. This is different from the photodissociation of the CH_2ICl at 193 nm in which case also the CH_2Cl radical and Cl atom are formed in significant yield. It is also known that Cl atoms react rapidly with CH_2ICl to produce CH_2Cl and ICl.[31] However, about half (0.46 ± 0.04) of the I atoms formed in the 248 nm photodissociation of the CH_2I_2 are known to be in excited state ($I(^2P_{1/2})$ or I* in channel (5b)) while the rest are produced in the ground state ($I(^2P_{3/2})$ or I) according to the channel (5a).[16] Unfortunately, nitrogen is inefficient quencher of the I* with a small room-temperature quenching rate coefficient, $k(N_2) = 6.5 \times 10^{-17}$ cm^3 s^{-1}, and helium is even less efficient than N_2.[32,33] The recorded signal at $m(I) = 127$ u showed very fast decay to almost constant value after 248 nm photodissociation of the CH_2I_2 in the absence of the reactant. The addition of NO_2 to the gas mixture clearly caused formation of I atoms as the product of the $CH_2I + NO_2$ reaction. The recorded signal at $m(I) = 127$ u, which was composed of I-atom formation in the photolysis and in the reaction, was however slightly distorted due to the excited iodine atoms produced in the photodissociation process (5b). Formation of NO was also measured, but due to the production of other radicals than CH_2I (CD_2I) in the photolysis or in the secondary chemistry and their possible reactions with NO_2 to produce NO, it was impossible to assign the origin of NO unambiguously only to the CH_2I (CD_2I) + NO_2 reaction. Other potential products of this reaction that were searched for but not detected include CH_2IO, IO, CHIO, HIO, HNO, HNO_2, HI, and INO.

For the reaction of the CH_2Br radical with NO_2, the detected product was also formaldehyde (or CD_2O when CD_2Br_2 was used as a precursor) as well as NO, whose origin was again difficult to assign quantitatively only to reaction 2. Search of products of the $CH_2Br + NO_2$ reaction was performed using dibromomethane as the precursor. Other potential products that were searched for but not observed include CH_2BrO, BrO, HNO, BrNO, HBrO, CH_2BrNO_2, CH_2BrONO_2, and HNO_2.

The detected product of the $CHBrCl + NO_2$ reaction was CHClO. The formation profile of CHClO is shown in the lower right corner of Figure 1. Again, the formation of NO was measured with the same problems as explained above. For the $CHBrCl + NO_2$ reaction, other potential products which were searched for but not detected include CHBrClO, CHBrO, $CHBrClNO_2$, $CHBrClONO_2$, BrNO, HNO, HBrO, BrO, and HNO_2.

For the detected primary products of the $R + NO_2$ reactions, the growth rates of the products matched those of the R decay rates in the reactions with NO_2 within about 1σ uncertainties. In addition, when products were searched for, it was also confirmed that no other radicals were formed in the photolysis or in the fast secondary reactions, which could have produced these primary products in reactions with NO_2. Employing this procedure, primary products of reactions 1−3 could be separated from the products of the secondary reactions. However, this method does not give information on product yields, which were not quantitatively measured in this work. Other potential products were also searched for. However, the absence of a measurable ion signal in these cases cannot be taken as a proof of the insignificance of these possible products in reactions 1−3 because the sensitivity of our experimental system is not known for all these species.

Measurements were carried out at different pressures to investigate possible contributions of three-body processes. Varying pressures between 2 and 6 Torr (He) did not change bimolecular rate coefficients in any of the $R + NO_2$ reactions studied. Therefore, no fast three-body processes are likely to be present in any significant extent in these reactions, which is consistent with previous investigations of the $CH_2Cl + NO_2$, $CHCl_2 + NO_2$, and $CCl_3 + NO_2$ reactions.[8] No secondary kinetic isotope effect ($k(CD_2X + NO_2)/k(CH_2X + NO_2$, X = I, Br) was observed above the experimental uncertainty for the $CH_2I + NO_2$ and $CH_2Br + NO_2$ reactions (Table 1, *i* and *k*). This is in accordance with previous observations in the $CH_2Cl + NO_2$ reaction.[8]

Preliminary propositions on the possible mechanisms of the (halogenated) methyl radical reactions with nitrogen dioxide can be made by combining current and previous information on the rate coefficients, products, and temperature dependencies of these reactions. The magnitude and the negative temperature dependency of the measured rate coefficients suggest that these radical−radical reactions proceed without any notable energy barrier to form a collision complex, for example via N- or O-atom attack of the NO_2 on the radical center. The potential energy surface of the $CH_3 + NO_2$ reaction given by Biggs et al.[34] and Yamaguchi et al.[35] for various reaction pathways include both N- and O-atom attack of the NO_2 on the carbon atom, while Zhang et al.[36] have obtained interaction only between N atom of the NO_2 and the C atom of the methyl radical. The energized methyl nitrite (CH_3ONO) can then decompose to bimolecular products via transition state(s) located energetically below the reactants, while energized nitromethane (CH_3NO_2) dissociates back to the reactants, collision stabilizes, or possibly overcomes high barrier(s) for rearrangements.[34−36] This is also consistent with the recent studies of Wollenhaupt et al.[37] and Kukui et al.[38] on the $CH_3 + NO_2$ reaction, where both bimolecular and termolecular reaction channels have been observed. According to the study of Wollenhaupt et al.,[37] there is an increase of about 40% in the reaction rate coefficient as the pressure is changed from 1 to 5 Torr near the low-pressure limit of the termolecular channel at room temperature. If similar or larger pressure dependencies had occurred in the current

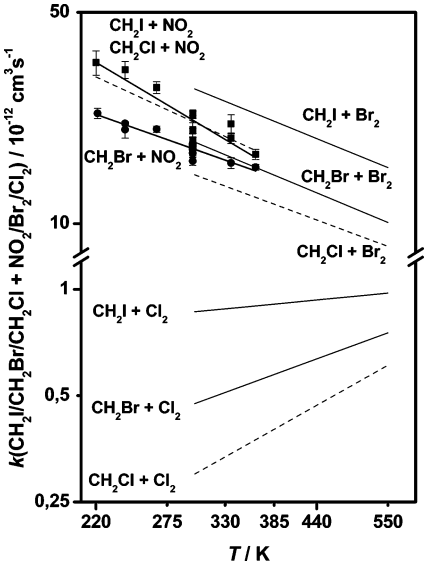

Figure 3. Comparison of bimolecular rate coefficients of the monohalogenated methyl radical (CH_2I, CH_2Br, and CH_2Cl) reactions with NO_2, Br_2, and Cl_2. Single measurements along with error bars and obtained fittings are shown for the current reactions ($CH_2I + NO_2$, $CH_2Br + NO_2$). For the other systems, including $CH_2Cl + NO_2$ reaction,[8] only the fitted lines are plotted for clarity. Data of the CH_2I, CH_2Br, and CH_2Cl radical reactions with Br_2 and Cl_2 are taken from the refs 44 and 45 and have been refitted to show in the $k = A \times (T/300\ \mathrm{K})^n$ form for the purpose of this work. Fittings of the $CH_2Cl + NO_2$, $CH_2Cl + Br_2$, and $CH_2Cl + Cl_2$ reactions are shown with dashed lines. Note the break in the vertical axis.

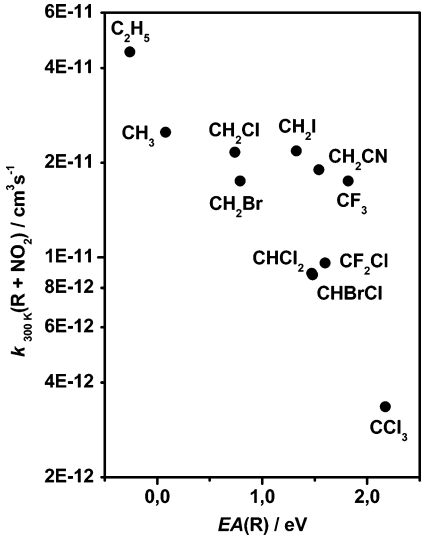

Figure 4. Plot of $R + NO_2$ reaction rate coefficients at 300 K vs adiabatic EA(R) involving substituted methyl radicals (CH_3,[48] C_2H_5,[14] CH_2CN,[14] CF_3,[11] CH_2Cl,[8] $CHCl_2$,[8] CCl_3,[8] and CF_2Cl[13]) shown in filled circles including current results. Values for the radical adiabatic electron affinities are taken from ref 21 except for CH_2I and CHBrCl, which are taken from refs 49 and 47, respectively.

measurements, this should have been observed. On the other hand, no pressure dependency was observed in the range 1.5−110 Torr of Ar and N_2 for the $CF_3 + NO_2$ reaction by Breheny et al.,[11] while the rate of the $CH_3 + NO_2$ reaction[37] more than doubled in this same density range. In both of these reactions bimolecular channels clearly dominate overall reaction rates under the low-pressure conditions, and it is very likely that this is also true for the reactions of the current study. In the $CH_3 + NO_2$ reaction, the most feasible bimolecular pathway leads to $CH_3O + NO$ products.[34,35] If halogenated methoxy radicals are products of the reactions studied in this work, it is highly probable that those species rapidly decompose to observed carbonyl compounds and halogen atoms.[39,40]

Rate coefficients of the monohalogenated methyl radical ($R_m = CH_2I$, CH_2Br, and CH_2Cl) reactions with NO_2, Br_2, and Cl_2 versus temperature are shown in Figure 3. Comparing the rate coefficients of these reactions, it can be seen that while $R_m + NO_2$ and $R_m + Br_2$ reactions are about equally fast and show the negative temperature dependency, $R_m + Cl_2$ reactions are significantly slower and possess positive temperature dependency. This indicates that $R_m + Cl_2$ reactions have a moderate reaction barrier while $R_m + NO_2$ and $R_m + Br_2$ reactions have a small or no barrier. Comparing the reactivity of the R_m radicals with the above reactants, it can be seen from the Figure 3 that in the $R_m + Br_2$ and $R_m + Cl_2$ reactions the order of reactivity is $CH_2I > CH_2Br > CH_2Cl$. However, in the case of the $R_m + NO_2$ reactions the order of reactivity is $CH_2I \approx CH_2Cl > CH_2Br$. Currently we do not have an explanation for this behavior.

Several experimental studies indicate that reactivity in the homologous series of radical/molecule reactions correlate with the ionization potential (IP) of the species that is the electron-donating in the transition state and with the electron affinity (EA) of the electron-withdrawing species.[7,41−43] For example, Miyoshi et al.[42] have obtained a good linear correlation for the alkyl and hydroxyalkyl radical reactions with O_2 by plotting $\log(k_{300\ \mathrm{K}})$ vs IP(R). Similarly, Paltenghi et al.[41] have observed a linear relationship for the alkyl radical reactions with O_2 and O_3 by plotting $\log(k_{300\ \mathrm{K}})$ vs IP(R) − EA(O_2 or O_3). Consequently, we also plotted $\log(k_{300\ \mathrm{K}})$ vs IP(R) − EA(NO_2), but no correlation was observed in our case. Instead, a linear relationship was obtained when $\log(k_{300\ \mathrm{K}})$ vs EA(R) was plotted. This is shown in Figure 4 for several substituted methyl radicals (CH_3, C_2H_5, CH_2CN, CF_3, CH_2Cl, $CHCl_2$, CCl_3, and CF_2Cl) in addition to the current results. In this case IP(NO_2) is a constant and was omitted for simplicity. A clear correlation for these mainly halogen-substituted methyl radicals can be observed. Similar deviations from the $\log(k_{300\ \mathrm{K}})$ vs IP−EA relationship have also been observed previously for the $R + Br_2$[44] and $R + Cl_2$[45] reactions, when R is a halogen-substituted methyl radical. However, as far as R = CH_3, C_2H_5, *i*-C_3H_7, or *t*-C_4H_9, i.e. only the alkyl radical, this correlation holds.[45,46] Thus it seems that the halogen substitution in the methyl radical breaks down the $\log(k_{300\ \mathrm{K}})$ vs IP(R)−EA(NO_2) relationship. Finally, it is interesting to observe that $CHCl_2$ and CHBrCl radicals, which have essentially the same EA = 1.472 eV,[47] also possess essentially the same reaction rates under the employed conditions, as shown in Figure 2. Additional kinetic studies are in progress to improve our understanding of the reactivities of substituted alkyl radicals.

Conclusions

The bimolecular rate coefficients of the $CH_2I + NO_2$, $CH_2Br + NO_2$, and $CHBrCl + NO_2$ reactions have been measured, and they obey the following temperature dependencies: $k(CH_2I + NO_2) = (2.18 \pm 0.07) \times 10^{-11} (T/300\ \mathrm{K})^{-1.45 \pm 0.22}$ cm^3 molecule^{-1} s^{-1}, $k(CH_2Br + NO_2) = (1.76 \pm 0.03) \times 10^{-11} (T/300\ \mathrm{K})^{-0.86 \pm 0.09}$ cm^3 molecule^{-1} s^{-1}, and $k(CHBrCl + NO_2) = (8.81 \pm 0.28) \times 10^{-12} (T/300\ \mathrm{K})^{-1.55 \pm 0.34}$ cm^3 molecule^{-1} s^{-1}. Formaldehyde (CD_2O) has been detected as a product for the CH_2I (CD_2I) + NO_2 and CH_2Br (CD_2Br) + NO_2 reactions. In the $CH_2I + NO_2$ reaction, formation of I atom and iodonitromethane (CH_2INO_2) or iodomethyl nitrite (CH_2IONO) products have also been observed. Formyl chloride (CHClO) has been detected as a product of the $CHBrCl + NO_2$ reaction.

There is no experimental evidence on the activation barrier or pressure dependence for any of the reactions studied.

Acknowledgment. A.J.E. thanks the Kone Foundation for research grants. R.S.T. also acknowledges support from the Bioscience and Environmental Research Council of the Academy of Finland and Maj and Tor Nessling Foundation, and the NoNeCK (Nordic Network for Chemical Kinetics).

References and Notes

(1) Geppert, W. D.; Eskola, A. J.; Timonen, R. S.; Halonen, L. *J. Phys. Chem. A*, **2004**, *108*, 4232.
(2) Knyazev V. D.; Slagle I. R. *J. Phys. Chem.*, **1995**, *99*, 2247.
(3) Eskola A. J.; Timonen R. S. *Phys. Chem. Chem. Phys.* **2003**, *5*, 2557.
(4) Atkinson D. B.; Hudgens J. W. *J. Phys. Chem. A* **1999**, *103*, 4242.
(5) Hahn D. K.; Klippenstein S. J.; Miller J. A. *Faraday Discuss.* **2001**, *119*, 79.
(6) Platz, J.; Nielsen, O. J.; Wallington, T. J.; Ball, J. C.; Hurley, M. D.; Straccia, A. M.; Schneider, W. F.; Sehested, J. *J. Phys. Chem. A* **1998**, *102*, 7964.
(7) Donahue, N. M. *Chem. Rev.* **2003**, *103*, 4593.
(8) Eskola, A. J.; Geppert, W. D.; Rissanen, M. P.; Timonen, R. S.; Halonen, L. *J. Phys. Chem. A* **2005**, *109*, 5376.
(9) Nesbitt, F. L.; Payne, W. A.; Stief, L. J. *J. Phys. Chem.* **1989**, *93*, 5158.
(10) Pagsberg, P.; Munk, J.; Anastasi, C.; Simpson, V. J. *J. Phys. Chem.* **1989**, *93*, 5162.
(11) Breheny, C.; Hancock, G.; Morrell, C. *Phys. Chem. Chem. Phys.* **2000**, *2*, 5105.
(12) Pagsberg, P.; Jodkowski, J. T.; Ratajczak, E.; Sillesen, A. *Chem. Phys. Lett.* **1998**, *286*, 138.
(13) Slagle, I. R.; Gutman, D. *J. Am. Chem. Soc.* **1982**, *104*, 4741.
(14) Park, J.-Y.; Gutman, D. *J. Phys. Chem.* **1983**, *87*, 1844.
(15) Kwok, W. M.; Phillips, D. L. *Chem. Phys. Lett.* **1997**, *270*, 506.
(16) Baughcum, S. L.; Leone, S. R. *J. Chem. Phys.* **1980**, *72*, 6531.
(17) Mössinger, J. C.; Shallcross, D. E.; Cox, R. A. *J. Chem. Soc., Faraday Trans.* **1998**, *94*, 1391.
(18) Butler, L. J.; Hintsa, E. J.; Shane, S. F.; Lee, Y. T. *J. Chem. Phys.* **1987**, *86*, 2051.
(19) Ji, L.; Tang, Y.; Zhu, R.; Tang, B.; Zhang, B. *Chem. Phys.* **2005**, *314*, 173.
(20) Bilde, M.; Wallington, T. J.; Ferronato, C.; Orlando, J. J.; Tyndall, G. S.; Estupiñan, E.; Haberkorn, S. *J. Phys. Chem. A* **1998**, *102*, 1976.
(21) Linstrom, P. J.; Mallard, W. G. Eds.; *NIST Chemistry WebBook, NIST Standard Reference Database Number 69, March 2003*, National Institute of Standards and Technology, Gaithersburg MD, 20899 (http://webbook.nist.gov).
(22) Borrell, P.; Cobos, C. J.; Luther, K. *J. Phys. Chem.* **1988**, *92*, 4377.
(23) Atkinson, R.; Baulch, D. L.; Cox, R. A.; Crowley, J. N.; Hampson, R. F.; Hynes, R. G.; Jenkin, M. E.; Rossi, M. J.; Troe, J. *Atmos. Chem. Phys.*, **2004**, *4*, 1461.
(24) Harwood: M. H.; Jones, R. L. *J. Geophys. Res.* **1994**, *99*, 22955.
(25) Sisk, W. N.; Miller, C. E.; Johnston, H. S. *J. Phys. Chem.* **1993**, *97*, 9916.
(26) Mueller, J. A.; Morton, M. L.; Curry, S. L.; Abbatt, J. P. D.; Butler, L. J. *J. Phys. Chem. A* **2000**, *104*, 4825.
(27) Kaufman, F. *Proress in Reaction Kinetics*; Porter, G., Ed.; Pergamon: New York, 1961; Vol. 1, p 1.
(28) Sun, F.; Glass, G. P.; Curl, R. F. *Chem. Phys. Lett.* **2001**, *337*, 72.
(29) Atkinson, R.; Baulch, D. L.; Cox, R. A.; Hampson, R. F., Jr.; Kerr, J. A.; Troe, J. *J. Phys. Chem. Ref. Data* **1992**, *21*, 1125.
(30) Teruel, M. A.; Dillon, T. J.; Horowitz, A.; Crowley, J. N. *Phys. Chem. Chem. Phys.* **2004**, *6*, 2172.
(31) Bilde, M.; Sehested, J.; Nielsen, O. J.; Wallington, T. J.; Meagher, R. J.; McIntosh, M. E.; Piety, C. A.; Nicovich, J. M.; Wine, P. H. *J. Phys. Chem. A* **1997**, *101*, 8035.
(32) Deakin, J. J.; Husain, D. *J. Chem. Soc., Faraday 2* **1972**, *68*, 41.
(33) Donovan, R. J.; Husain, D. *Trans. Faraday Soc.* **1966**, *62*, 1050.
(34) Biggs, P.; Canosa-Mas, C. E.; Fracheboud, J.-M.; Parr, A. D.; Shallcross, D. E.; Wayne, R. P.; Caralp, F. *J. Chem. Soc. Faraday Trans.* **1993**, *89*, 4163.
(35) Yamaguchi, Y.; Teng, Y.; Shimomura, S.; Tabata, K.; Suzuki, E. *J. Phys. Chem. A* **1999**, *103*, 8272.
(36) Zhang, J.-X.; Liu, J.-Y.; Li, Z.-S.; Sun, C.-C. *J. Comput. Chem.* **2005**, *26*, 807.
(37) Wollenhaupt, M.; Crowley, J. N. *J. Phys. Chem. A* **2000**, *104*, 6429.
(38) Kukui, A.; Bossoutrot, V.; Laverdet, G.; Le Bras, G. *J. Phys. Chem. A* **2000**, *104*, 935.
(39) Orlando, J. J.; Tyndall, G. S.; Wallington, T. J. *J. Phys. Chem.* **1996**, *100*, 7026.
(40) Bilde, M.; Sehested, J.; Nielsen, O. J.; Wallington, T. J. *J. Phys. Chem. A* **1997**, *101*, 5477.
(41) Paltenghi, R.; Ogryzlo, E. A.; Bayes, K. D. *J. Phys. Chem.* **1984**, *88*, 2595.
(42) Miyoshi, A.; Matsui, H.; Washida, N. *J. Phys. Chem.* **1990**, *94*, 3016.
(43) Masaki, A.; Tsunashima, S.; Washida, N. *J. Phys. Chem.* **1995**, *99*, 13126.
(44) Timonen, R. S.; Seetula, J. A.; Niiranen, J.; Gutman, D. *J. Phys. Chem.* **1991**, *95*, 4009.
(45) Seetula, J. A.; Gutman, D.; Lightfoot, P. D.; Rayes, M. T.; Senkan, S. M. *J. Phys. Chem.* **1991**, *95*, 10688.
(46) Timonen, R. S. *Ann. Acad. Sci. Fenn. Ser. A2* **1988**, *218*, 5.
(47) Born, M.; Ingemann, S.; Nibbering, N. M. M. *Int. J. Mass Spectrom. Ion Processes* **2000**, *194*, 103.
(48) Yamada, F.; Slagle, I. R.; Gutman, D. *Chem. Phys. Lett.* **1981**, *83*, 409.
(49) Born, M.; Ingemann, S.; Nibbering, N. M. M. *J. Am. Chem. Soc.* **1994**, *116*, 7210.